Springer

Journal of Mechanical Science and Technology 23 (2009) 2583~2591

Journal of Mechanical Science and Technology

www.springerlink.com/content/1738-494x
DOI 10.1007/s12206-009-0801-x

Landing impact analysis of sports shoes using 3-D coupled foot-shoe finite element model †

Jin-Rae Cho[1,2], Seung-Bum Park[3,*], Sung-Hyun Ryu[1], Sung-Ho Kim[1] and Shi-Bok Lee[1]

[1] *School of Mechanical Engineering, Pusan National University, Busan 609-735, Korea*
[2] *Research Institute of Midas Information Technology Co. Ltd., Gyeonggi-Do 462-807, Korea*
[3] *Busan Economic Promotion Agency, Footwear Industrial Promotion Center, Busan 618-820, Korea*

(Manuscript Received November 26, 2007; Revised April 6, 2009; Accepted July 1, 2009)

Abstract

The rapid spread of various sports games has changed the role of shoes from the simple protection of human feet to more advanced ones like competency improvement. Accordingly, intensive research efforts are being focused on the development of high-competency sports shoes by taking kinesiology and biomechanics into consideration. However, the success of this goal depends definitely on the reliable evaluation of the main functions required for sports shoes. As the first part of our study on the landing impact analysis of court sports shoes, this paper introduces a coupled foot-shoe finite element model in order to fully reflect the mutual interaction between the foot and the shoe, not relying on traditional independent field experiments any more. Through illustrative numerical experiments, we assess the reliability of the proposed coupled FEM model by comparing with the experimental results and investigating the fundamental landing impact characteristics of sports shoes.

Keywords: Sports shoes; Coupled foot-shoe model; Landing impact; Finite element analysis; Ground reaction force; Center of pressure; Acceleration and frequency

1. Introduction

In the past, the role of shoes was to protect human feet from unexpected injuries during walking, running or jumping, because human feet are inherently subjected to various reaction forces by the ground during such foot motions. However, advances in the footwear industry and the rapid spread of various sports games have changed the role of shoes to playing competency. In sports such as tennis, marathon, basketball and volleyball, the competency depends on the shoe quality. The major aspects of sports shoes influencing the competency of sports players are function, comfort, durability, weight and so on.

A sports shoe is mostly composed of outsole, midsole, insole, upper and several reinforcements. Though, its detailed shape and construction are different for different sports shoes depending on the playing conditions and the dominant foot motions [1]. In this context, the design concept of shoes can not be unified and the shoe components must be designed so as to compatible with the sport. In addition, the influences of gender, body conditions, and playing technique of the player can not be disregarded [2]. Thus, the design of high-performance sports shoes depends on the evaluation accuracy of the major aspects required for each sports game.

Roughly speaking, the research on sports shoes dates from the 1930s even though the methodologies at that time were not comparable to the current ones, relying mostly on subjective intuition. But, since late 1970s, these studies have been expanded and evolved into the fields of kinesiology, biomechanics and sports medicine by many subsequent investigators.

† This paper was recommended for publication in revised form by Associate Editor Young Eun Kim
*Corresponding author. Tel.: +82 51 979 1800, Fax.: +82 51 7979 1729
E-mail address: sbpark@kfiglobal.or.kr

Clarke et al. [3] investigated the effects of shoe design parameters and the ground stiffness on the characteristics of running. On the other hand, Hennig et al. [4] introduced the capacitive method to obtain a visualized foot-print pressure distribution from the analog signals. Cavanagh and Lafortune [5] analyzed the ground reaction force by applying biomechanics. Whereas, Frederick [6] analyzed the kinematics of leg and foot motions and applied to the shoe design. Later, the advances in sensor/video camera, image processing system and material testing equipment realized not only the analysis of the detailed and quick locomotion of human leg and foot [2] but also the accurate estimation the material properties of bone, tissue and shoes components [7].

The finite element method was also employed to limb biomechanics [8] and footwear science [9, 10]. But, most of these studies were focused on the deformation and stress in individual bones, knee joints and shoe components, and the loading conditions were set arbitrarily or relied on experimental data. However, when the research is aimed at the shoe design and evaluation, the most important concern should be to accurately evaluate ground-shoe and shoe-foot interactions. It is because the numerical analysis accuracy and the shoe design quality are substantially influenced by the reliability of the impact characteristic evaluation. Traditionally, these interaction effects have been measured through experiments and taken into the uncoupled numerical simulation as loading conditions. This indirect approach is not only time-/cost-consuming but also painstaking to accomplish since a huge amount of experimental data is required. More recently, Asai and Murakami [11] introduced 3-D ground-foot interaction models to resolve this problem. However, these interaction models are still insufficient to accurately evaluate the impact characteristics of sports shoes because the ground-shoe-foot interaction has not been fully considered.

In this context, the goal of this paper is to introduce a coupled 3-D foot-shoe finite element model [12] in order to fully and accurately reflect the ground-shoe-foot interaction. 3-D foot-leg and shoe models are constructed by considering the major bones, joints, tissues and shoes components, and the interaction between both models is coupled by the surface-to-surface contact algorithm [13]. Through illustrative numerical experiments, the efficiency and reliability of the proposed model are demonstrated and the major landing impact characteristics of court sports shoes are investigated.

2. Problem description

2.1 Landing impact and its evaluation

Foot motions in every sports game are accompanied with the landing event, even though its posture and occurrence frequency depend on the type of game. The impact intensity is usually measured by the impact force (or the ground reaction force) which is a dynamic force resulting from the interaction between the foot and the ground. It can be observed from Fig. 1(a) that the landing impact not only gives rise to the direct shock to the foot but also transfers up to the human head through the lower extremity. The inherent viscous damping of the human foot absorbs the impact force and attenuates its transfer intensity to some extent [14], but the damage and the injury occurrence possibility become considerably higher when the player is in motion without wearing sports shoes.

Landing impact characteristics like the peak impact force, the loading rate and the center of pressure are dependent on various parameters, such as shoes, foot shape, landing posture, motion velocity, body and ground conditions, and so on. Hence, the evaluation of such characteristics is of great importance for the understanding of the impact mechanism and its transfer through the human body. The reduction of unexpected damages and injuries of the lower extremity can be accomplished by using data from such dies. Furthermore, it has recently become an essential procedure in shoe design according to the need of high-quality sports shoes which can maximize the comfort and playing competency [15]. However, since the reliable evaluation of landing impact characteristics is

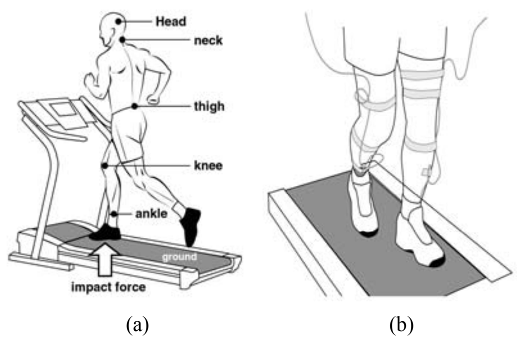

(a) (b)

Fig. 1. Illustration: (a) landing impact and its transfer; (b) experiment scene.

not simple but complex it has been traditionally per formed by experiments with the help of the specially designed experiment apparatus illustrated in Fig. 1(b).

Meanwhile, shoe design based upon the impact characteristics evaluation requires a correlation between the shoe design parameters and the major shoe performances. Thus, parametric experiments with respect to impact characteristics and shoe performances are indispensable. In this regard, a reliance on experiments may encounter several limitations in the development of high-quality sports shoes which are currently characterized by frequent model change and shorter development period, in aspects of cost and time. The inherent limitations of experimental methods can be overcome by the finite element method, provided they are validated.

2.2 Lower limb and sports shoes

As depicted in Fig. 2(a), the human foot is composed of a number of bones, cartilages, tendons and ligaments which are embedded into the underlying tissue in highly complicated composition structure. Furthermore, each component exhibits inherent anisotropic viscoelastic behavior. Therefore, the construction of a detailed simulation model of the human foot is complicated due to the complex structural composition, the joint motions and the nonlinear material behavior. From the biomechanics point of view, relative motions of several joints such as ankle, subtalar are controlled by tendons as well as ligaments, and are important because such motions are essential to describe the kinematics of the foot skeleton. Meanwhile, the soft tissue and skin characterize the shock absorption and the load transfer through human body on impact. Due to these complexities, the numerical analyses associated with the foot landing impact have been traditionally performed with simplified foot models, such as a simple rigid bone-hyperelastic tissue model [16], a 3-D skeleton model without considering the soft tissue [11].

Referring to Fig. 2(b), a sports shoe consists of an outsole, mid-sole, insole, upper, shoe lace and several functional parts like heel cap and arch supporter. The outer surface of the outsole is grooved in specific pattern to improve the traction performance on the ground. On the other hand, the other two soles absorb the major portion of the landing impact while both upper sole and shoe lace influence the fitness and the contact intensity between shoe and foot. The specific

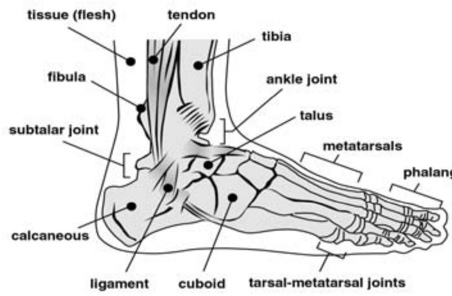

(a)

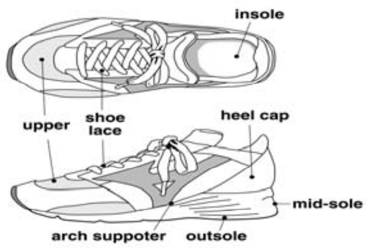

(b)

Fig. 2. Schematic view: (a) leg and foot; (b) sports shoe.

functions depending on the type of sports are achieved by inserting the appropriately designed functional parts. Compared to the human foot, the mechanical properties of shoe components can be rather easily determined by means of specially designed material testing devices. However, the construction of a 3-D full shoe model in which individual parts are reflected in detail requires not only elaborate modeling efforts but also a tremendous number of finite elements. Additionally, the coupling between foot and shoe models considerably increases the complexity and CPU time of the numerical simulation. Nevertheless, a coupled 3-D foot-shoe model is prerequisite to secure both the effectiveness and reliability of the numerical evaluation of landing impact characteristics.

3. 3-D coupled foot-shoe FEM model

Fig. 3(a) represents the finite element models of the lower limb skeleton and soft tissue, where the skeleton model, which is constructed with 4-node tetrahedron elements, is largely composed of two bone assemblies and a combined joint. It can be observed from Fig. 3(b) that the tibia and fibula are modeled as a single bone, while the other bones as another bone assembly. The minor joints, except for ankle and sub-

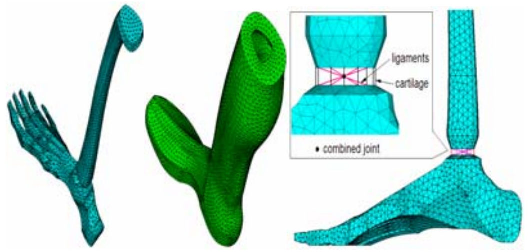

(a) (b)

Fig. 3. Finite element models: (a) skeleton and soft tissue; (b) ankle and subtalar joints.

talar ones, have been neglected. Two main joints are modeled as a combined joint composed of a rigid ball, several ligament link and cartilage beam elements, so that the separated two bone assemblies freely rotate relatively to each other with the appropriate rotational rigidity. The soft tissue model is also generated with 4-node tetrahedron elements, and its inner surface is carved such that the outer surface of the lower limb skeleton completely contacts with the tissue model. As both meshes are separately generated, their mesh discretization patterns are not compatible along the common interface, requiring the surface-to-surface tying algorithm [12] to simulate their interaction. Bones, tissue, ligaments and cartilages are assumed to be linearly isotropic.

Referring to Fig. 4(a), three soles are modeled with 4-node tetrahedron elements while 3-node shell elements are used for upper. Since the outsole is manufactured with rubber-like materials, its hyperelastic behavior is modeled by the five-term Moonley-Rivlin model, with the strain energy density functional W defined by

$$W\left(C_{ij}, I_i\right) = C_{10}\left(I_1 - 3\right) + C_{01}\left(I_2 - 3\right) + C_{11}\left(I_1 - 3\right) \times \left(I_2 - 3\right) + C_{20}\left(I_1 - 3\right)^2 + C_{30}\left(I_3 - 3\right)^3 \quad (1)$$

Note that the material constants C_{ij} are determined by least-square fitting of experimental values. We use the Blatz-Ko form model [17] in order to describe the mechanical behavior of mid-sole and insole which are manufactured with compressible polyurethane rubbers. The strain energy density functional W of this model is given by

$$W\left(I_1, I_2, I_3\right) = G\left(I_2 / I_3 + 2\sqrt{I_3} - 5\right) / 2 \quad (2)$$

The assembled finite element model of the court sports shoes is represented in Fig. 4(b), where each

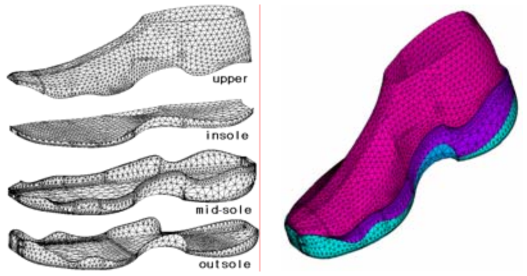

(a) (b)

Fig. 4. Finite element modeling of sports shoes: (a) shoe parts; (b) assembly.

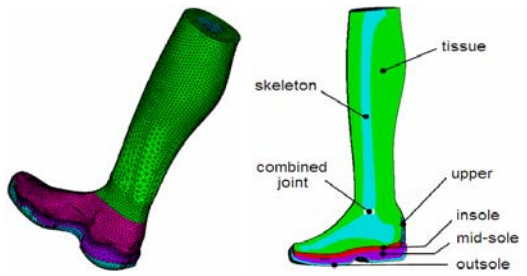

(a) (b)

Fig. 5. Coupled 3-D foot-shoe model: (a) finite element mesh; (b) schematic representation.

shoe part is completely bonded to its adjacent parts by using the node-to-node tying method. For this, FEM meshes of each shoe part are constructed such that the mesh distributions of two adjacent parts are exactly the same along the common surface. The shoe model is constructed so that its inner surface is in appropriate contact with the outer surface of the soft tissue model. The interaction between foot and shoes is treated by imposing the frictional surface-to-surface contact, and the frictional coefficient μ between foot and shoes is set by 0.5 [18].

Figs. 5(a) and 5(b) show the final coupled 3-D foot-shoe finite element model and the schematic representation of its structural composition, respectively. The most prominent feature of this state-of-the-art model is the realization of the lower limb wearing the sports shoes, so that any kind of foot motion that can occur in actual sports events can be simulated with perfect freedom. This model is highly distinguished from the conventional simulation models which are not only simplified and restricted but also rely on experimental data for accounting for the interaction effects between foot and shoes. As can be observed from Fig. 5(b), the relative rotational motion of both foot and shoes with respect to the combined joint is resisted by the stiffness of the ligament links, the cartilage beams and the soft tissue. The pre-compression by the shoe laces is not considered for this coupled model, but its effect on the landing impact evaluation is not considerable. Furthermore, the viscoelastic behavior of the low extremity is not considered because the main goal of the current study is to examine the validity of our 3-D coupled foot-shoe model.

4. Numerical experiments

A vertical straight landing event of a human foot from $h = 300mm$ above ground with the zero initial velocity is taken for the landing impact simulation. The total weight of the human body is set by $60kgf$ and its dynamic effect is reflected by adding the total body mass to the mass center of the foot-shoe coupled model, as depicted in Fig. 6. To shorten the total CPU time, the actual landing simulation starts from the vertical position of $5mm$ just above the ground, by specifying the initial velocity $V_{ini} = \sqrt{2gh} = 2.405m/s$ to the foot-shoe coupled model. A frictional dynamic analysis was carried out by the 3-D explicit finite element method [19], for which the frictional coefficient μ between the outsole and the ground and the penalty parameter k_p for the material incompressibility are set by 0.5 and $10MPa$, respectively.

The material properties and the numbers of finite elements which are taken for each part in the impact simulation model are recorded in Table 1. Where, the clay ground is discretized uniformly with 8-node cubic elements and the fixed boundary condition is specified to its entire bottom surface. Meanwhile, the outsole is discretized with 6,574 4-node tetrahedron elements and the material constants involved in the Moonley-Rivlin model in Eq. (1) are as follows: $C_{10} = -0.00149$, $C_{01} = 0.11732$, $C_{11} = -0.00182$, $C_{20} = 0.01720$ and $C_{30} = 0.02$. It can be noted that the material properties of bone, tissue, ligament and cartilage were chosen by referring to Dai, et al. [18] and Yamada [20]. While the others were determined by uni-axial tension experiments using shoe component specimens, incorporated with the least-square curve fitting technique.

The landing simulation was performed in $0.05\sec$ after the initial contact of outsole with the ground. Fig. 7(a) compares the time histories of the ground reaction force (GRF) between FEM and experiment. As mentioned earlier, the experiment was performed on an AMTI force platform [2, 21], with the same conditions as the numerical simulation such as the body weight, the landing height and the ground stiffness and the friction coefficient. As a whole, the numerical prediction is in a good agreement with the experiment such that the peak value occurs at the same time $t = 0.036\sec$. One noticeable difference is that the numerical prediction does not show the oscillation after the peak, which is because the inherent viscous

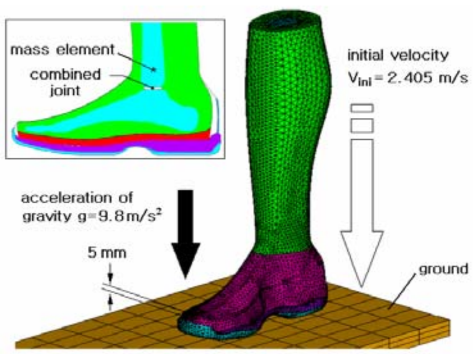

Fig. 6. Loading and boundary conditions for the example.

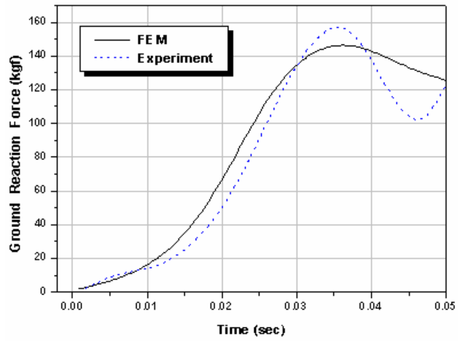

(a)

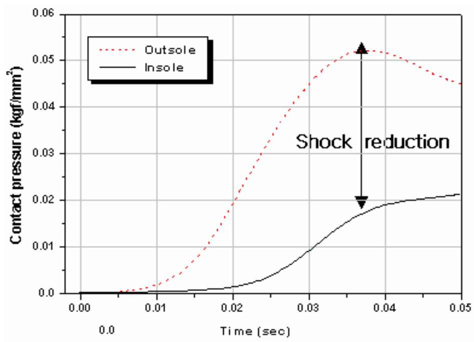

(b)

Fig. 7. Time histories: (a) GRF; (b) peak contact pressures at outsole and insole.

Table 1. Material properties of lower limb and sports shoes (except for outsole).

Components	Young's modulus $E\,(MPa)$	Poisson's ratio ν	Mass density $\rho\,(kg/m^3)$	Element number
Bone	7,500	0.34	1,500	21,656
Tissue	1.15	0.49	9,500	82,578
Ligament (links)	11.5	0.34	-	37
Cartilage (beams)	10.0	0.34	-	6
Upper	11.76	0.35	9,400	2,865
Insole	1.98	0.35	2,300	4,797
Mid-sole	2.49	0.35	2,300	19,997
Ground	10	0.36	-	300

damping of soft tissue and sports shoes is not considered in the numerical analysis. The peak value of $148kgf$ corresponds to 2.7 times of the total body weight, which is consistent with the report by Mann and Hagy [1] that the relative peak GRF with respect to the total body weight generally becomes 2-3 BW.

Fig. 7(b) compares the time histories of the peak contact pressures produced at the outsole and insole. Differing from the outsole, the peak contact pressure at insole shows a uniform increase with the lapse of time after the peak point, even though the slope increase is not significant. When focused on the time $t = 0.036\sec$, the peak contact pressures are as follows: $0.0564 kgf/mm^2$ at outsole and $0.0187 kgf/mm^2$ at insole. Thus, the difference in the peak pressures occurring at both soles is $0.0377 kgf/mm^2$, so that the relative impact absorption by outsole and mid-sole reaches 67%.

Fig. 8(a) depicts the seven sub-regions of the outsole which are conventionally used to evaluate the regional peak pressures resulting from the collision between the outsole and the ground. The experimental results were obtained by the traditional EMED testing method [22]. Referring to Fig. 8(b), the comparison confirms that the present coupled foot-shoe model produces acceptable numerical accuracy. One noticeable fact is that the numerical simulation overestimates the peak pressure in the rear-foot region but underestimates in the fore-foot region, which is caused by the limitation in the modeling of ankle and subtalar joints and in the accurate determination of the rotational stiffness of the combined joint.

Distributions of the equivalent strain at five major model parts are represented in Figs. 9(a)-9(e), when the ground reaction force reaches the peak value. It can be realized that relatively larger deformations occurred at insole and mid-sole owing to the lower

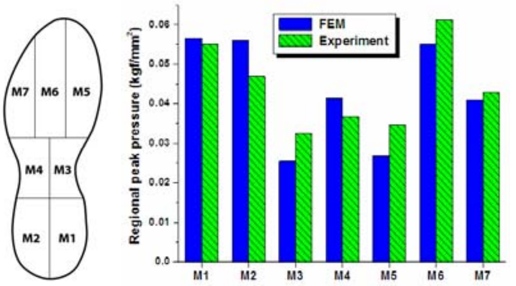

(a) (b)

Fig. 8. Regional peak pressures at outsole: (a) sub-regions; (b) comparison with experiment.

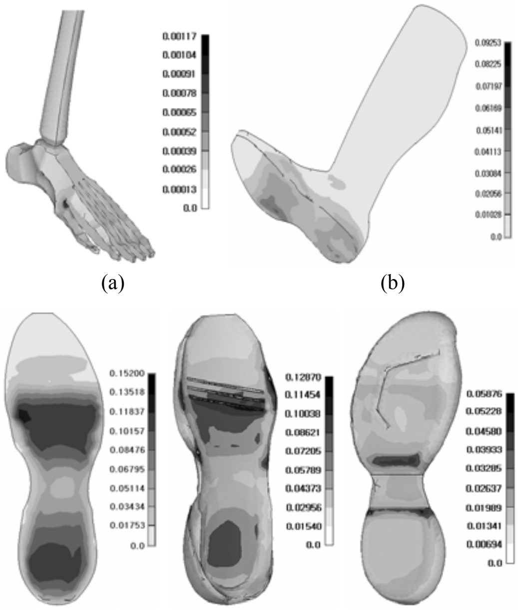

(c) (d) d)

Fig. 9. Equivalent strain at $0.0036\sec$ after impact: (a) bone; (b) tissue; (c) insole; (d) mid-sole; and (e) outsole.

stiffness than that of the outsole. As well as, the impact absorption from insole to foot is clearly observed,

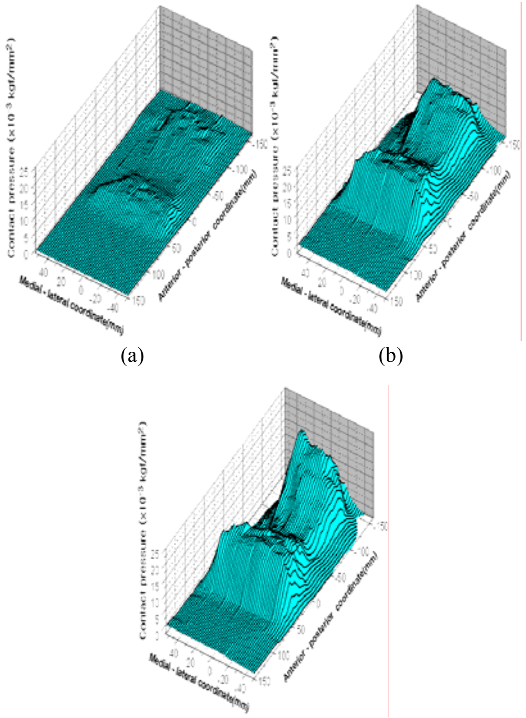

Fig. 10. Contact pressure distributions at insole: (a) $0.005\,\text{sec}$; (b) $0.015\,\text{sec}$; and (c) $0.036\,\text{sec}$.

because soft tissue with the lowest stiffness shows a peak strain which is smaller than that of the insole. Contact pressure distributions within the insole at three different time stages are represented in Figs. 10(a)-10(c). At the time $t = 0.036\,\text{sec}$, the peak contact pressure is $0.0167 kgf / mm^2$ and it shows a good agreement with the experimental value of $0.0163 kgf / mm^2$.

It is important to note that the direct and simultaneous prediction of the dynamic responses of individual components of foot and sports shoes is the major advantage of the present coupled foot-shoe model, because it is not possible by various kinds of the traditional uncoupled separate simulation models presented in the Introduction.

Fig. 11 represents the locus of the center of pressure within the insole during the entire landing event. The center of pressure $(\bar{x}, \bar{y})$ is calculated, by using the nodal pressure values p_i at each finite element node (x_i, y_i), by

$$\bar{x} = \sum p_i x_i \Big/ \sum p_i, \quad \bar{y} = \sum p_i y_i \Big/ \sum p_i \tag{3}$$

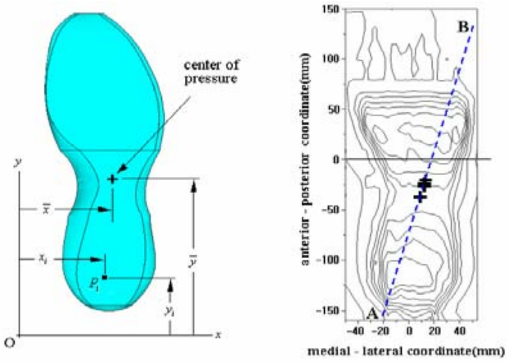

Fig. 11. Movement of the center of pressure during the landing motion.

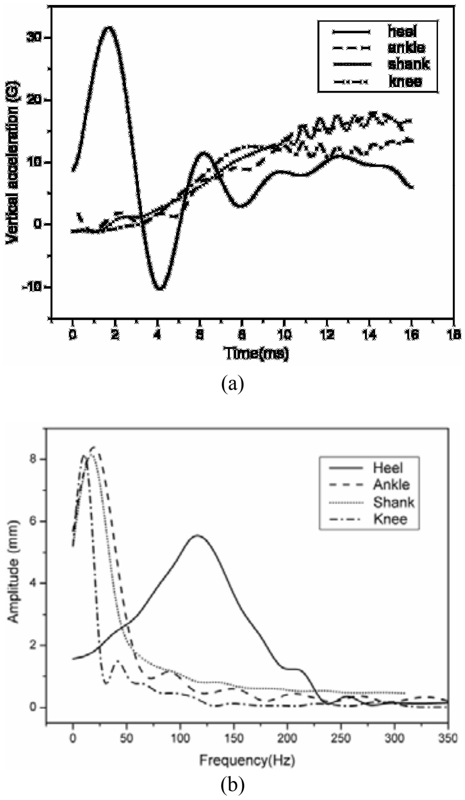

Fig. 12. Transfer of the landing impact: (a) vertical acceleration; (b) frequency.

The dotted line connecting two points A and B indicates the reference line for evaluating the movement of the center of pressure. In other words, landing instability and over-pronation do not occur when the center of pressure moves along this reference line. From the numerical results, we found that the deviation of the center of pressure from the reference line is

Table 2. Peak accelerations (G) and central frequencies (Hz) at four different positions.

Item	Heel	Ankle	Shank	Knee	RR*
Peak acceleration	32.5	17.2	16.9	14.1	56.6
Center frequency	117.4	25.1	24.7	13.5	88.5

RR: Relative reduction (%) = (Heel-Knee)/Heel*100%

negligible, not resulting in undesired injury caused by the over-pronation. The detailed maximum movement of the center of pressure is as follows: $3.49mm$ in the medial-lateral direction and $14.30mm$ in the anterior-posterior direction.

Fig. 12(a) represents the time histories of the vertical accelerations at four different positions of the leg-foot model, heel, ankle, shank and knee. As depicted in Fig. 1(a), the acceleration sensors are attached to the skin of a human leg and foot, so that the measurement points are set in accordance with the experiment. The heel exhibits the severe fluctuation in the vertical acceleration with large amplitude just after the landing impact, but the extreme transient response decays with the lapse of time. On the other hand, three other positions show a gradual increase in the vertical acceleration without any remarkable fluctuation. It can be observed from Table 2 that the peak acceleration decreases in proportion to the distance from the landing impact position such that the relative reduction from heel to knee reaches 56.6%.

The frequency responses evaluated at four different positions are compared in Fig. 12(b), where the heel shows a wide frequency band with a relatively high center frequency. However, both the frequency band and the central frequency significantly reduce as the measurement position moves away from the impact position, with the relative reduction of the center frequency equal to 88.5% from heel to knee. From the acceleration time histories and the frequency responses, one can confirm that the landing impact at the heel is significantly absorbed by the lower extremity.

5. Conclusion

A fully coupled 3-D foot-shoe finite element model has been introduced in this paper, for the accurate and effective numerical implementation of the foot-shoe-ground interaction in the landing event. The complex bone geometry, the ankle and subtalar joints were considered in the modeling of the lower limb skeleton. Subsequently, the skeleton model was assembled into the soft tissue model. In addition, essential parts of sports shoes were realistically modeled and assembled by using the node-to-node or surface-to-surface tying technique. The final 3-D foot-shoe model was generated by combining the foot model and the shoe model according to the frictional surface-to-surface contact.

The validity and reliability of the proposed coupled model have been examined through the illustrative numerical simulation of the vertical straight landing event. The GRF time-history and the regional peak pressures at outsole that were predicted by the 3-D frictional dynamic impact analysis showed a good agreement with the experimental results. Furthermore, a comparison of the peak contact pressures at the insole between FEM and experiment justified the accuracy of the present method. Several other important aspects associated with the landing event, such as the equivalent stain distribution, the time histories of the contact pressure and the vertical acceleration and the frequency response, were investigated by the proposed coupled model with perfect freedom.

References

[1] R. A. Mann and J. Hagy, Biomechanics of walking, running and sprinting, *American J. Sports Medicine*, 8 (1980) 345-350.

[2] P. R. Cavanagh, *Biomechanics of Distance Running*, Human Kinetics Books, Champaign, IL, USA, (1990).

[3] T. Clarke, E. C. Frederick and C. L. Hanmill, The effects of shoe design parameters on rearfoot control in running, *Medicine and Science in Sports and Exercise*, 15 (1983) 376-381.

[4] E. M. Hennig, P. M. Cavanagh and N. H. Mcmillan, Pressure distribution measurements by high precision piezoelectric ceramic force transducers, *Biomechanics VII-B (Eds. H. Matsui and K. Kobayashi)*, (1983) 1081-1088.

[5] P. R. Cavanagh and M. A. Lafortune, Ground reaction forces in distance running, *J. Biomechanics*, 13 (1980) 397-406.

[6] E. C. Frederick, Kinematically mediated effects of sports shoe design: a review, *J. Sports Science*, 4 (1986) 169-184.

[7] B. M. Nigg, W. Hertzog and L. J. Read, Effects of viscoelastic shoe insoles on vertical impact forces in

heel-toe running, *The American J. Sports and Medicine*, 16 (1988) 70-76.
[8] A. G. Godest, M. Beaugonin, E. Haug, M. Taylor and P. J. Gregson, Simulation of a knee joint replacement during a gait cycle using explicit finite element analysis, *J. Biomechanics*, 35 (2000) 267-275.
[9] T. Y. Shiang, The nonlinear finite element analysis and plantar pressure measurements for various shoe soles in heel region, *Proc. of the National Science Council, ROC, Part B: Life Sciences*, 21 (1997) 168-174.
[10] R. Verdejo and N. J. Mills, Heel-shoe interactions and the durability of EVA foam running-shoe midsoles, *J. Biomechanics*, 37 (2004) 1379-1386.
[11] T. Asai and H. Murakami, Development and evaluation of a finite element foot model, *Proc. of the 5th Symposium on Footwear Biomechanics (Eds. E. M. Hennig and A. Stacoff)*, (2001) 10-11.
[12] S. H. Kim, *Evaluation of Landing Impact Characteristics of Court Sports Shoes by Finite Element Method*, Masters Thesis, Pusan National University, Busan, Korea, 2005.
[13] J. R. Cho, K. W. Kim, W. S. Yoo and S. I. Hong, Mesh generation considering detailed tread blocks for reliable 3D tire analysis, *Adv. Eng. Softw.*, 35 (2004) 105-113.
[14] J. Denoth, Load on the locomotor system and modeling, *Biomechanics of Running Shoes (Eds. B. Nigg)*, (1986) 63-116.
[15] T. G. McPoil, Athletic footwear: design, performance and selection issues, *J. Science and Medicine in Sport*, 3(3) (2000) 260-267.
[16] D. Lemmon, T. Y. Shiang, A. Hashmi, J. S. Ulbrecht and P. R. Cavanagh, The effect of insoles in therapeumatic footwear: a finite element approach," *J. Biomechanics*, 30 (1997) 615-620.
[17] P. J. Blatz and W. L. Ko, Application of finite element theory to the deformation of rubbery materials, *Trans. Soc. Rheol.*, 6 (1962) 223-251.
[18] X. Q. Dai, Y. Li, M. Zhang and J. T. M. Cheung, Effect of sock on biomechanical responses of foot during walking, *Clin. Biomech.*, 21 (2006) 314-321.
[19] J. R. Cho, K. W. Kim, D. H. Jeon, and W. S. Yoo, Transient dynamic response analysis of 3-D patterned tire rolling over cleat, *Eur. J. Mech. A/Solids*, 24 (2005) 519-531.
[20] H. Yamada, *Strength of Biological Materials*, Williams & Wilkins, Baltimore, USA, (1970).
[21] E. Y. Suda, A. F. Amorim and I. C. N. Sacco, I.C.N., 2009, Influence of ankle functional instability on the ankle electromyography during landing after volleyball blocking, *J. Electromyogr. Kinesiol.*, 19 (2009) 84-93.
[22] Z. Nakhaee, A. Rahimi, M. Abaee, A. Rezasoltani and K. Khademi Kalantari, The relationship between the height of the medial longitudinal arch (MLA) and the ankle and knee injuries in professional runners, *The Foot*, 18 (2008) 84-90.

Jin-Rae Cho received his B.S. degree in Aeronautical Engineering from Seoul National University in 1983. He then received his M.S. and Ph.D. degrees from University of Texas at Austin in 1993 and 1995, respectively. He served as an Editor of KSME International Journal and Journal of Mechanical Science and Technology. Dr. Cho is currently a vice director of the Research Institute of Midas IT Co. Ltd. Dr. Cho's current research interests include computational tire mechanics, fluid-structure interaction, functionally graded materials, footwear biomechanics, and nonlinear finite element programming.

Seung-Bum Park received his B.S. degree in Phsical Education from Pusan National University, Korea, in 1993. He obtained his M.S. and Ph.D in biomechanics from the Pusan National University. Dr. Park is a head of Footwear Biomechanics Team in the Footwear Industrial Promotion Center in Busan, South Korea, while serving as an Executive Board Member of International Footwear Biomechanics Group. His role at the institute is to support Korean footwear industry by collaborating with universities, corporations and other research institutes in the field of footwear biomechanics. His research is focusing specifically on the footwear design not only for providing benefits in biomechanical factors (i.e. muscle activation and joint loading) but for improving the safety and athletic performances related to lower limb biomechanics and neuromuscular response.